J. Fluid Mech. (1973), *vol.* 57, *part* 1, *pp.* 129–148
Printed in Great Britain

A model of flow separation at a free surface

By M. S. LONGUET-HIGGINS

Department of Applied Mathematics and Theoretical Physics,
University of Cambridge and National Institute of Oceanography,
Wormley, Godalming, Surrey

(Received 2 October 1970 and in revised form 28 July 1972)

Flow separation can be observed (1) at the leading edge of a spilling breaker or 'white-cap', (2) at the lower edge of a tidal bore or hydraulic jump and (3) upstream of an obstacle abutting a steady free-surface flow. At the point of flow separation there is a discontinuity in the slope of the free surface. The flow upstream of this point is relatively smooth; the flow downstream of the discontinuity is turbulent.

In this note, a local solution for the flow in the neighbourhood of the discontinuity is derived. The turbulence is represented by a constant eddy viscosity N, and the tangential stress across the interface between the laminar and turbulent zones is expressed in terms of a drag coefficient C. It is shown that the inclinations of the free surface of the two sides of the discontinuity depend on C only, and are independent of N and g. As C increases from zero to large values, so the inclination of the free surface in the turbulent zone increases from 10° 54′ to 30°. In the laminar zone the inclination of the free surface simultaneously decreases from 10° 54′ to 0°, the densities in the two zones being assumed equal.

Owing to the possible entrainment of air at the separation point, the effective density ρ' in the turbulent zone may be less than the density ρ in the laminar zone. When these densities are allowed to be different it is found that the possible flows are of two distinct types. Flows of the first type, called 'quasi-static', are contiguous to a state of rest. Flows of the second type, called 'dynamic', are contiguous with the frictional flows described above, for which $\rho' = \rho$. At a given positive value of C there exists generally only one quasi-static solution. There is also just one dynamic solution provided $\rho'/\rho > 0{\cdot}50012$. On the other hand, if $\rho'/\rho < 0{\cdot}5$ there may be either two or no dynamic flows, depending on the value of C; and when $0{\cdot}5 < \rho'/\rho < 0{\cdot}50012$ there may be three such flows.

The inclination of the free surface is studied as a function of C and ρ'/ρ.

1. Introduction

The breaking of surface waves has important dynamical consequences in the ocean, both in deep and in shallow water. In deep water, white-caps may be responsible for a high proportion of wave energy dissipation (see Stewart & Grant 1962), and hence for the conversion of wave momentum to larger scales of motion. Thus if D denotes the mean rate of energy dissipation per unit horizontal area, and if c is the phase velocity of the breakers, an amount of wave momentum

equal to D/c is available for conversion to larger scales of motion, including mean currents.

The turbulence due to breaking waves is probably also the chief agent of vertical mixing and for vertical transfer of heat and momentum in the uppermost layers of the ocean, while the entrainment of air by breaking waves must influence the transfer of dissolved gases between atmosphere and ocean.

Likewise in shallow water it is known that longshore currents, which transport large quantities of sand and sediment parallel to the coastline, are generated within the surf zone by waves striking the coast at an oblique angle (Galvin 1967). The mean tangential stress τ exerted by the waves is equal to $(D/c)\sin\theta$, where D and c have the same meanings as before and θ denotes the angle of incidence (see Longuet-Higgins 1970*a*, *b*). Though most of the dissipation in the surf zone is due to breaking waves, neither the form of the breaking waves, nor the distribution of turbulence with depth are well known.

Indeed, while the theory of surface waves *of small amplitude* has been highly developed (see, for example, Lamb 1932) and much progress has been made with the theory of weakly nonlinear interactions (Phillips 1966), our knowledge of breaking waves is surprisingly scanty.

It was shown by Stokes (1880) that a steady progressive wave of limiting amplitude must have a sharp crest with a discontinuity of 60° in surface slope. Using this criterion, the limiting form of waves in deep water was determined by Michell (1893) and in shallow water by McCowan (1894), Davies (1952) and others. Numerical calculations of unsteady waves have also been successfully carried out by, for example, Street (1972) up to the point of breaking. But little, if any work has been done on the analytical description of a gravity wave *after it has broken*. The reason is no doubt connected with the fact that such flows are essentially turbulent, and potential theory is no longer applicable to the whole flow.

Laboratory studies of breaking waves in shallow water have been published by Mason (1952), Iverson (1952), Ippen & Kulin (1955), Divoky, Le Méhauté & Lin (1970), and others. Mason (1952) distinguished two types of breaking wave: on the one hand 'plunging breakers', in which the wave crest topples forwards and falls violently onto itself; and on the other hand 'spilling breakers', in which the free surface becomes unstable near the wave crest and forms a quasi-steady white-cap on the forward slope of the wave. Illustrations of these two types are given in figures 1 and 2 of Mason (1952).

In contrast, a considerable amount of experimental work has been done on hydraulic 'jumps' in channel flows; for a comprehensive review see Rajaratnam (1967). These are essentially shallow-water flows. The flow in the jump has been explored in its dependence on the Froude number. Evidently some experimental difficulties remain to be overcome, in particular those arising from the entrainment of air at the free surface. Quantitative measurements by Rajaratnam (1962) indicate that the mean density in a vertical section can fall as low as $0{\cdot}8\,\mathrm{g/cm^3}$, and possibly lower.

It must be emphasized, however, that breakers are by no means a shallow-water phenomenon, as is shown by the presence of white-caps in deep water

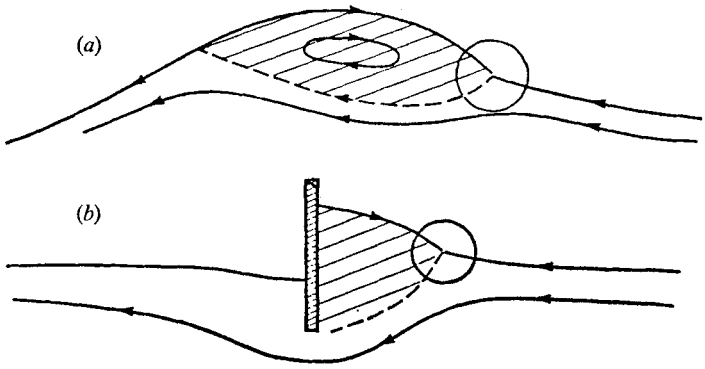

FIGURE 1. Examples of flow separation. (*a*) A spilling breaker. (*b*) The flow induced by an obstacle at the surface of a steady stream.

(Monahan 1971). Generally they seem to occur when the vertical acceleration approaches the limiting value $\frac{1}{2}g$ (Longuet-Higgins 1969*a*). It is also certain that the extreme shearing motion near the crests of large-scale waves will sometimes give rise to a shearing instability.

In deep water there are at least two ways in which waves may attain their limiting amplitude. The first occurs when the frequency spectrum is narrow. Since the phase velocity of deep-water waves is twice that of their group velocity, the amplitude of waves will grow to a maximum and then decay as they pass through their wave envelope. Near the maximum amplitude they may break.

The second mechanism applies when the shorter waves riding on the backs of longer waves are forced by the latter to steepen and break near the crests of the longer waves (Longuet-Higgins 1969*b*).

In deep water, white-caps appear generally to last for a shorter time than on gently sloping beaches, but from visual observation white-caps may be better classed as 'spilling' than as 'plunging'. Some observations of white-caps are given in a recent note by Donelan, Longuet-Higgins & Turner (1972).

The complete analytical description of breaking waves, and of hydraulic jumps, presents a challenging task. In the present paper we do not attempt a complete description of either of these phenomena, but we suggest on the other hand a possible model for one local feature of such flows, namely the flow near the forward edge of a spilling breaker or hydraulic jump, where the turbulent flow meets the more tranquil water (see figure 1). In this region the flow is evidently turbulent, as elsewhere in the breaker. We suggest that it may be treated as a turbulent wedge with a certain eddy viscosity whose magnitude is determined by conditions outside the local flow (see figure 2). Such a local solution is developed in the present paper.

In § 2 we show that the only type of smooth irrotational flow which can sustain a discontinuity of surface gradient is one with an angle of 120° – in fact, a generalization of the Stokes 120° angle flow (see figure 2). But to sustain this the fluid on

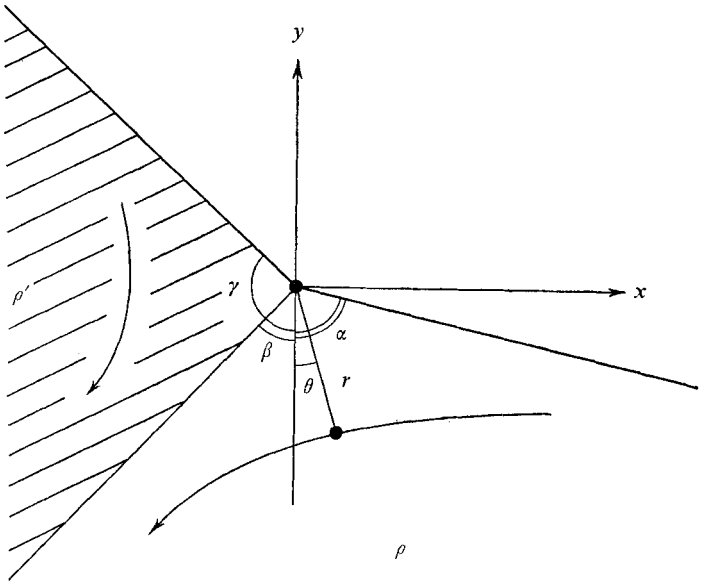

FIGURE 2. Co-ordinates and notation for the assumed flow.

the left of the discontinuity must be at rest, and the free surface on the left must be horizontal. There is no way to support a rise in water level on the left, except by frictional forces, or (in turbulent motion) by Reynolds stresses.

We therefore assume (in § 3) that the fluid on the left of the discontinuity is turbulent, and is dominated by Reynolds stresses. The latter are assumed to be represented by a coefficient N of eddy viscosity. The *mean* velocity in the turbulent zone is assumed small compared to the flow on the right (in a frame of reference travelling with the phase velocity). Across the boundary of separation, both normal and tangential stresses are balanced, the tangential stresses on the left being given by a constant coefficient C times the square of the velocity on the right. At the free surface, both components of stress vanish. Under these conditions it is shown that a local two-dimensional solution does exist. Moreover it has the remarkable property that the inclination of the free surface on the two sides of the discontinuity depends only upon C, and is independent of both N and g. The angle of elevation on the left is shown to lie between 10° 54′ and 30°; the angle of depression on the right is between 10° 54′ and zero. Various special cases are discussed in § 4.

In § 5 we discuss the effect of a possible difference in density on the two sides of the interface, caused by the entrainment of air at the point of separation. The flows described above are generalized so as to include an arbitrary ratio of the densities, and the effect on the inclination of the free surface is determined.

A comparison with some observations of the flow in hydraulic jumps is made in § 6.

In the discussion in § 7 it is suggested that a way may be opened up to treat the hitherto intractable problem of breaking waves, and more generally, of mixed turbulent and laminar free-surface flows. In such analyses the present local

solution may be an essential feature, representing the flow near the point of separation.

2. A frictionless flow

By choosing a reference frame moving with a suitable horizontal velocity we may reduce the motion to a steady flow. Let polar co-ordinates be taken as in figure 2, with the origin at the point of discontinuity and with the line $\theta = 0$ directed vertically downwards. Let the boundary of the fluid on the right be given by $\theta = \alpha$, that on the left by $\theta = -\gamma$, with a possible interface at $\theta = -\beta$. Let p and g denote the pressure and gravitational acceleration, and ρ and ρ' the densities on the right and left respectively.

Let us first suppose the flow to be irrotational. Then, in an incompressible fluid, we seek a stream function ψ such that

$$\nabla^2\psi = 0 \tag{2.1}$$

with boundary conditions

$$\left.\begin{array}{lll} \psi = 0, \quad p = 0, & \text{when} & \theta = \alpha, \\ \psi = 0, \quad p \text{ continuous}, & \text{when} & \theta = -\beta, \\ \psi = 0, \quad p = 0, & \text{when} & \theta = -\gamma. \end{array}\right\} \tag{2.2}$$

We may, or may not, have a discontinuity in $\partial\psi/\partial\theta$ at $\theta = -\beta$. Following Stokes (1880) we try

$$\psi = Ar^n \sin n(\theta - \alpha) \quad (-\beta < \theta < \alpha). \tag{2.3}$$

This satisfies the first condition at the surface $\theta = \alpha$. To satisfy the second condion we note that in steady frictionless flow

$$p/\rho - gr\cos\theta + \tfrac{1}{2}q^2 = \text{constant} \tag{2.4}$$

by Bernoulli's theorem. Since from (2.3)

$$q^2 = n^2 A^2 r^{2n-2} \tag{2.5}$$

we have

$$p = \rho(gr\cos\theta - \tfrac{1}{2}n^2A^2r^{2n-2}) + \text{constant}. \tag{2.6}$$

The vanishing of p on $\theta = \alpha$ then implies that

$$n = \tfrac{3}{2}, \tag{2.7}$$

so that the angle between radial streamlines must be 120°, and further

$$A^2 = \tfrac{8}{9}g\cos\alpha, \tag{2.8}$$

so that if $A \neq 0$, then $\cos\alpha > 0$; in other words, the streamlines must slope *downwards* from the origin. This is also clear from the fact that the velocity has to vanish at the origin, and a particle on a surface of constant pressure can gain kinetic energy only by going downhill.

If now we try to satisfy the free-surface conditions at $\theta = -\gamma$ by the expression $\psi = Br^n \sin n(\theta + \gamma)$, $-\gamma < \theta < -\beta$, we find, by a similar argument that either $\gamma < \frac{1}{2}\pi$, which is obviously impossible when $0 < \alpha < \frac{1}{2}\pi$, or else $B = 0$, that is to say the fluid on the left is stationary. Then the free surface on the left is horizontal ($\gamma = \frac{1}{2}\pi$).

Can we satisfy the boundary conditions on the interface $\theta = -\beta$? On the left the pressure is simply the hydrostatic pressure $p = \rho' g r \cos\beta$. On the right the pressure is given by equation (2.6), which, in view of (2.8), may be written as

$$p = \rho g r (\cos\beta - \cos\alpha). \tag{2.9}$$

Equating p and p' on the two sides of $\theta = -\beta$ we have

$$\rho' \cos\beta = \rho(\cos\beta - \cos\alpha), \tag{2.10}$$

or, since $\alpha + \beta = \frac{2}{3}\pi$,

$$(\rho - \rho')\cos\beta = \rho \cos(\tfrac{2}{3}\pi - \beta). \tag{2.11}$$

This leads immediately to

$$(\rho - \rho')/\rho = \tfrac{1}{2}\sqrt{3}\tan\beta - \tfrac{1}{2} \tag{2.12}$$

and hence

$$\tan\beta = (3\rho - 2\rho')/\sqrt{3}\rho. \tag{2.13}$$

The two extreme cases are as follows. First, when $\rho' = 0$, then

$$\alpha = \beta = \tfrac{1}{3}\pi, \quad A = \pm\tfrac{2}{3}g^{\frac{1}{2}}. \tag{2.14}$$

This is the Stokes 120° angle (Stokes 1880). Secondly, when $\rho' = \rho$ then

$$\alpha = \tfrac{1}{2}, \quad \beta = \tfrac{1}{6}\pi, \quad A = 0. \tag{2.15}$$

The free surface on the right is then horizontal and no flow takes place. Intermediate values of the density ratio ρ'/ρ give flows which have non-zero values of A and which are in effect generalizations of the Stokes 120° angle flow. All these have a discontinuity in velocity on the surface $\theta = -\beta$, and all have a horizontal free surface on the left.

We remark that if a non-zero vorticity (without friction) is allowed in the flow on either side of the discontinuity, it will not affect the angle of the free surface. For ψ is then the sum of a harmonic function plus a solution ψ_0 of the equation

$$\nabla^2\psi_0 = -\omega_0, \tag{2.16}$$

where ω_0 is the limiting vorticity near the corner. But since in radial co-ordinates

$$\nabla^2 \equiv \left(\frac{1}{r}\frac{\partial}{\partial r}\right)\left(r\frac{\partial}{\partial r}\right) - \left(\frac{1}{r}\frac{\partial}{\partial\theta}\right)^2 \tag{2.17}$$

it follows that the relevant solution of (2.16) will be of order $\omega_0 r^2$, which tends to zero with r more rapidly than the harmonic function (2.3). Hence the presence of vorticity may affect the *curvature* of the free surface near the crest, but not the limiting angle. For the Stokes 120° angle this was pointed out by Miche (1944).

3. A turbulent flow

The observation that the free surface generally slopes upwards to the left of the discontinuity means that the flow there must be effected either by frictional forces or by Reynolds stresses, for without these it would be impossible for a particle at the free surface to be brought to rest at the origin (see equation (2.4)).

In this section, therefore, we shall seek a solution representing laminar flow on the right but highly turbulent flow on the left (see figure 2). For simplicity we

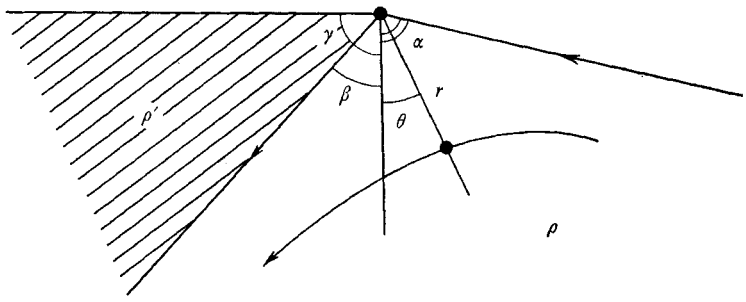

FIGURE 3. The local flow in a frictionless fluid with different densities.

shall first assume that the densities on the left and on the right are equal, i.e. $\rho' = \rho$.

Most turbulent flows are difficult to represent satisfactorily, the present being no exception. Moreover there are some outstanding differences between this and other types of flow, in that the source of the turbulence may be largely external to the region considered – in a breaking wave, for example, most of the turbulence may originate nearer to the wave crest. Secondly, the mean flow near the stagnation point must be relatively small to an observer moving with the phase velocity of the wave.

These considerations lead us to suggest a very simple model as follows. Let us suppose that the P_{ij} are given in terms of the mean flow $\overline{u}_i$ by expressions analogous to those for ordinary viscous stresses, that is to say

$$P_{ij} = \rho N \left(\frac{\partial \overline{u}_i}{\partial x_j} + \frac{\partial \overline{u}_j}{\partial x_i} \right) - P\delta_{ij}. \tag{3.1}$$

Here N is an eddy viscosity, which we shall at first assume to be constant. The quantity P is analogous to (but not equal to) the pressure p. We assume also that the Reynolds stresses dominate the inertia terms in the equations for the mean motion. Then in the turbulent zone we have essentially a balance between Reynolds stresses and gravity. The equations for the stream function $\overline{\psi}$ of the mean flow become, in rectangular co-ordinates,

$$\left.\begin{aligned} \frac{1}{\rho}\frac{\partial P}{\partial x} &= N\frac{\partial}{\partial y}(\nabla^2\overline{\psi}), \\ \frac{1}{\rho}\frac{\partial P}{\partial y} + g &= -N\frac{\partial}{\partial x}(\nabla^2\overline{\psi}) \end{aligned}\right\} \tag{3.2}$$

(y being directed vertically upwards). Cross-differentiation gives

$$\nabla^4\overline{\psi} = 0 \tag{3.3}$$

and we see also that $P/\rho + gy$ is the harmonic conjugate of $N\nabla^2\overline{\psi}$, the expression

$$(P/\rho + gy) + iN\nabla^2\overline{\psi} \tag{3.4}$$

being an analytic function of $x + iy$.

On $\theta = -\gamma$ we have the boundary conditions

$$\overline{\psi} = 0, \qquad P_{\theta\theta} = 0, \qquad P_{r\theta} = 0, \tag{3.5}$$

where now, in radial co-ordinates,

$$\left.\begin{aligned} P_{r\theta} &= \rho N\left[\left(\frac{1}{r}\frac{\partial}{\partial\theta}\right)^2 - \left(r\frac{\partial}{\partial r}\right)\left(\frac{1}{r}\frac{\partial}{\partial r}\right)\right]\overline{\psi}, \\ P_{\theta\theta} &= -2\rho N\frac{\partial}{\partial r}\left(\frac{1}{r}\frac{\partial}{\partial\theta}\right)\overline{\psi} - P \end{aligned}\right\} \tag{3.6}$$

(see, for example, Lamb 1932, p. 579).

At the interface $\theta = -\beta$, which separates the turbulent flow on the left from the laminar flow on the right, we shall assume that

$$\overline{\psi} = 0, \qquad P_{\theta\theta} = -p, \qquad P_{r\theta} = C\rho q^2, \tag{3.7}$$

where p and q denote the pressure and speed in the laminar flow; that is,

$$\left.\begin{aligned} p/\rho &= -gy - \tfrac{1}{2}q^2, \\ \tfrac{1}{2}q^2 &= gr\cos\alpha = gr\cos(\beta - \tfrac{2}{3}\pi). \end{aligned}\right\} \tag{3.8}$$

The second of the conditions (3.7) may therefore be written as

$$P_{\theta\theta}/\rho - gy = \tfrac{1}{2}q^2. \tag{3.9}$$

The third of equations (3.7) is based on the assumptions that (1) the *mean* flow on the left is small compared with that on the right, and (2) there is a small entrainment of fluid from the laminar flow into the turbulent flow. If we define an entrainment constant ϵ by

$$\epsilon = \frac{\text{normal velocity of laminar flow across boundary}}{\text{relative tangential velocity of laminar and mean turbulent flow}} \tag{3.10}$$

then conservation of momentum tangential to the boundary suggests that

$$C \doteqdot \epsilon. \tag{3.11}$$

In a recent review Turner (1969) has quoted evidence that, at the boundary of a square jet, ϵ is commonly of order 0·08. Hence we expect C to be of this order also.

It is remarkable that the above equations (2.1) and (3.3), with the boundary conditions (2.2), (3.5), (3.7) and (3.9), admit a simple exact solution. Let us take

$$\overline{\psi} = Er^3\sin 3(\theta+\gamma) + Fr^3\sin(\theta+\gamma), \tag{3.12}$$

where E and F are constants to be determined. Using (2.17) we have

$$\nabla^2\overline{\psi} = 8Fr\sin(\theta+\gamma), \tag{3.13}$$

which is a harmonic function, so (3.3) is satisfied. Moreover from (3.4) it follows that

$$P/\rho + gy = 8NFr\cos(\theta+\gamma). \tag{3.14}$$

Since $\overline{\psi}$ is an odd function of $\theta+\gamma$ we see that the two boundary conditions $\overline{\psi} = 0$

and $P_{r\theta} = 0$ on $\theta+\gamma = 0$ are automatically satisfied. In general we have from (3.6) and (3.12)

$$P_{r\theta}/\rho = -Nr[12E\sin 3(\theta+\gamma)+4F\sin(\theta+\gamma)]. \tag{3.15}$$

This obviously vanishes when $\theta+\gamma = 0$. We have also

$$P_{\theta\theta}/\rho - gy = -2Nr[6E\cos(\theta+\gamma)+2F\cos(\theta+\gamma)] - (P/\rho+gy) \tag{3.16}$$

or using (3.14)

$$P_{\theta\theta}/\rho - gy = -12Nr[E\cos 3(\theta+\gamma)+F\cos(\theta+\gamma)]. \tag{3.17}$$

The condition that $P_{\theta\theta}$ should vanish on $\theta = -\gamma$ now yields

$$E+F = -(g/12N)\cos\gamma \tag{3.18}$$

and the three conditions on $\theta = -\beta$ yield respectively

$$\left.\begin{aligned} E\sin 3\delta + F\sin\delta &= 0,\\ E\cos 3\delta + F\cos\delta &= -Q,\\ E\sin 3\delta + \tfrac{1}{3}F\sin\delta &= -2CQ,\end{aligned}\right\} \tag{3.19}$$

where we have written

$$\delta = \gamma-\beta \tag{3.20}$$

(which is the vertex angle of the turbulent 'wedge') and

$$Q = \frac{\frac{1}{2}q^2}{12Nr} = \frac{g}{12N}\cos(\tfrac{2}{3}\pi-\beta). \tag{3.21}$$

From the first and third of equations (2.19) it follows that

$$E = -3CQ/\sin 3\delta, \qquad F = 3CQ/\sin\delta \tag{3.22}$$

and so on substituting in the second of (3.19) we find, if $Q \neq 0$,

$$\cot 3\delta - \cot\delta = 1/3C. \tag{3.23}$$

Similarly on substituting in (3.18) and using (3.21) we find

$$\operatorname{cosec} 3\delta - \operatorname{cosec}\delta = \frac{1}{3C}\frac{\cos\gamma}{\cos(\frac{2}{3}\pi-\gamma+\delta)}. \tag{3.24}$$

Equations (3.23) and (3.24) constitute the solution to the problem. Given the drag coefficient C we may first use (3.23) to determine δ and then use (3.24) to determine γ and hence all the other parameters of the flow. The pattern of the streamlines is independent of both N and g.

4. Discussion of the solution

From (3.23) we have

$$\frac{1}{3C} = \frac{-\sin 2\delta}{\sin 3\delta\sin\delta} = \frac{-2\cos\delta}{\sin 3\delta}, \tag{4.1}$$

and so

$$C = -\tfrac{1}{6}\sin 3\delta\sec\delta. \tag{4.2}$$

This function is shown in figure 3. In the range $0 < \delta < \frac{1}{3}\pi$, it is negative and has a minimum equal to $-0{\cdot}196$ where

$$\cos 2\delta = \tfrac{1}{2}(\sqrt{3}-1), \quad \delta = 34^\circ 16'. \tag{4.3}$$

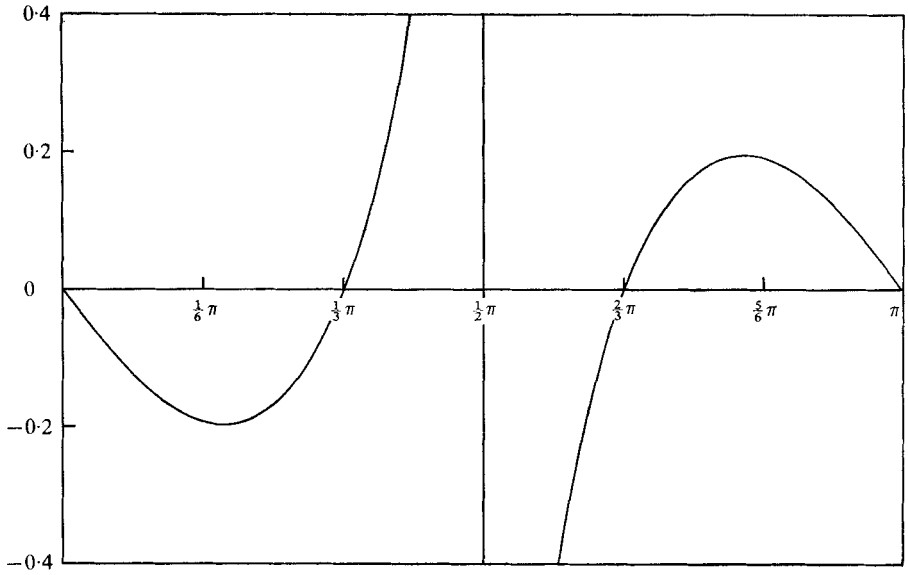

FIGURE 3. Graph of the function $f(\delta) = -\frac{1}{6}\sin 3\delta \sec \delta$, giving the drag coefficient C as a function of the angle δ at the apex of the turbulent wedge.

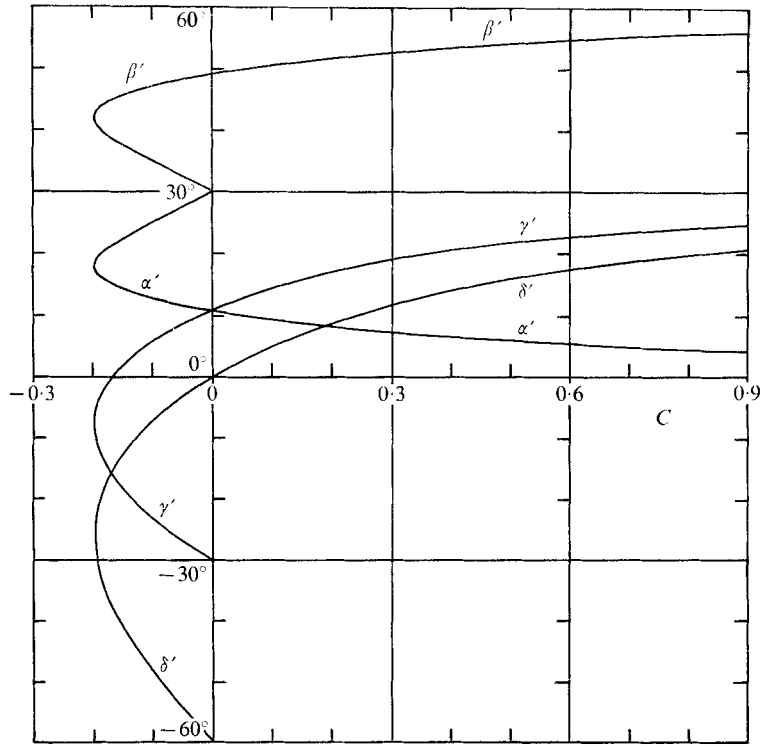

FIGURE 4. The angles of inclination α', β' and γ', and the angle δ' of the discontinuity in slope at the separation point, shown as functions of the drag coefficient C.

Since C is negative, this range $0 < \delta < \frac{1}{3}\pi$ corresponds to *upwards* flow along the interface.

When, on the other hand, $\frac{1}{3}\pi < \delta < \frac{1}{2}\pi$, C must be positive. Indeed, as $\delta \to \frac{1}{2}\pi$ so $C \to \infty$. But since in practice C is probably small, only those values of δ close to $\frac{1}{3}\pi$ are of interest. In this neighbourhood we have

$$C \doteq \delta - \tfrac{1}{3}\pi = \delta', \tag{4.4}$$

say. It will be noted that δ' is just equal to the discontinuity in the inclination of the free surface at $r = 0$.

Beyond the point $\delta = \frac{1}{2}\pi$, the roots of (4.2) do not yield physical solutions, since they imply (as will be seen) that $\alpha > \frac{1}{2}\pi$.

From (3.23) and (3.24) we have, on eliminating C, the relation

$$\frac{\cot 3\delta - \cot \delta}{\operatorname{cosec} 3\delta - \operatorname{cosec} \delta} = \frac{\cos(\frac{2}{3}\pi - \gamma + \delta)}{\cos \gamma} \tag{4.5}$$

relating δ and γ. Manipulation of both sides yields

$$\cos\delta/\cos 2\delta = \cos(\delta + \tfrac{2}{3}\pi) + \sin(\delta + \tfrac{2}{3}\pi)\tan\gamma \tag{4.6}$$

and hence

$$\tan\gamma = \tan 2\delta + 3^{\frac{1}{2}} \sec 2\delta. \tag{4.7}$$

This simple relation enables us at once to calculate γ in terms of δ, and hence also β and α. In figure 4 we have plotted, besides δ', the functions

$$\alpha' = \tfrac{1}{2}\pi - \alpha, \quad \beta' = \tfrac{1}{2}\pi - \beta, \quad \gamma' = \gamma - \tfrac{1}{2}\pi. \tag{4.8}$$

The angles α' and γ' represent the inclination of the free surface to the horizontal on the right and left respectively, and β' represents the inclination of the interface. From figure 4 it will be seen that as C increases from 0 to ∞, so δ' increases from 0° to 30°. At the same time α' *decreases* from 10° 54′ to 0°; β' increases from 49° 6′ to 60°, and γ' increases from 10° 54′ to 30°. We shall now discuss some special cases.

We take first some non-negative values of C (figures 5*a*, *b*, *c*). A typical flow is when $\delta = 75°$ (figure 5*b*). The flow is in the direction we might expect intuitively. The free surfaces on the left and right are inclined at angles of 21° (upwards) and 6° (downwards) respectively. As the drag coefficient is increased, so the flow approaches the configuration shown in figure 6(*c*). Although $C \to \infty$, the flow on the left remains bounded, since at the same time $q^2 \to 0$ in such a way as to make $C\rho q^2$ finite. In the limit, (3.22) shows that $E = F = 3CQ$, so that on the left

$$\overline{\psi} \propto r^3 \sin 2(\theta + \gamma) \sin(\theta + \gamma). \tag{4.9}$$

This represents a flow that is concentrated mainly in the neighbourhood of the interface.

As C moves in the opposite direction we pass through the limiting case $C = 0$, $\delta = 60°$, shown in figure 6(*a*). Paradoxically, the free surface is not horizontal in this case. The reason is that, although the tangential stress at the interface vanishes, the presence of the turbulence results in an increase of the normal stress $P_{\theta\theta}$ (hence a reduction in P) whose effect must be counterbalanced by a

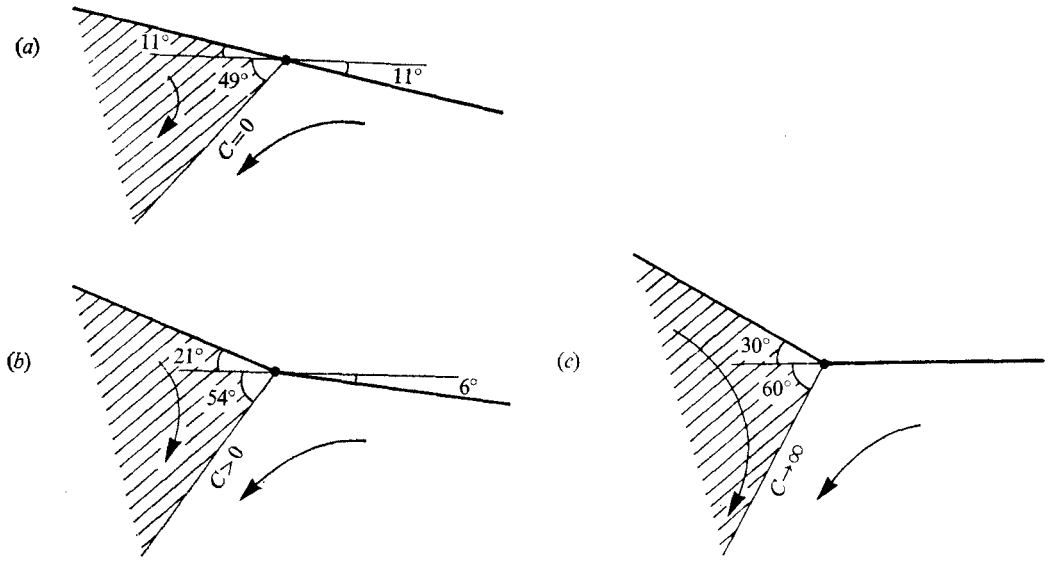

FIGURE 5. Flow configurations when $C \geqslant 0$: (*a*) $\delta = 60°$, (*b*) $\delta = 75°$, (*c*) $\delta = 90°$.

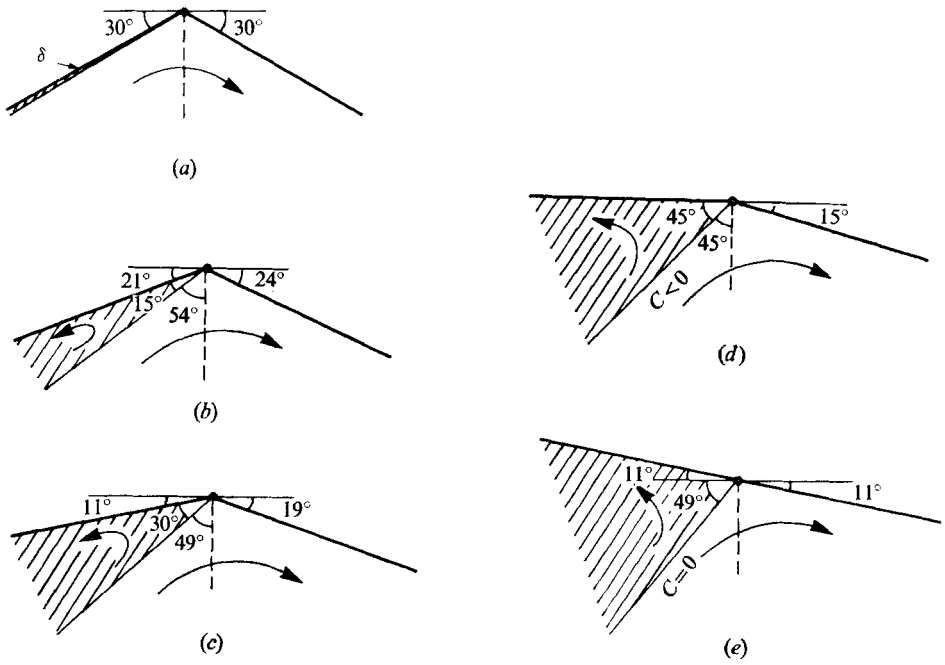

FIGURE 6. Flow configurations when $C = 0$: (*a*) $\delta \ll 1$, (*b*) $\delta = 15°$, (*c*) $\delta = 30°$, (*d*) $\delta = 60°$.

reduction in the pressure p on the right of the interface. Hence the flow on the right is similar to a special case of the frictionless flow described in § 2. The fluid on the left, however, is not stationary. Taking the limit of equations (3.22) as $C \to 0$ we find $E \neq 0$, $F \to 0$ and hence

$$\overline{\psi} \propto r^3 \sin 3(\theta + \gamma), \tag{4.10}$$

which represents a simple, irrotational flow in a 60° corner. By the symmetry of the flow it can be seen that this flow ensures the vanishing of $P_{r\theta}$ both on $\theta = -\beta$ and $\theta = -\gamma$.

Some solutions representing negative values of C are shown in figure 6. When $\delta \ll 1$ (figure 6*a*) the turbulent zone is very thin and the laminar flow approximates that in a Stokes 120° angle C is then small.† As δ increases so does $|C|$ until the maximum at $\delta = 34° 16'$. When $\delta = 45°$ the free surface on the left is horizontal, the mean flow being given by $E = -F = -3(2)^{\frac{1}{2}} CQ$, and so

$$\overline{\psi} \propto r^3 \sin 2(\theta + \gamma) \cos(\theta + \gamma). \tag{4.11}$$

Finally when $\delta = 60°$ we have the same flow as in figure 5 (*a*) except that the direction is reversed.

We note that in deriving (3.22) and (3.23) it was necessary to divide by Q, so that the solution $Q = 0$, hence $E = F = 0$ was excluded. This is the trivial solution in which the fluid is at rest on both sides of the interface. But we see that this solution is not continuous with either of the ranges examined above. This remark serves to emphasize the nonlinearity of the present flows. To establish them we must pass through some configuration other than a state of rest. Once established, however, observation suggests that they are at least securlarly stable.

5. Turbulent flow with differing densities

Any entrainment of air at the point of separation may be expected to reduce the effective density of the fluid above the interface; that is, in the turbulent region. The method of § 5 can also be applied to the problem when the density ρ' of the turbulent fluid on the left differs from the density ρ in the laminar region on the right. The drag coefficient C may be expected to depend upon the relative density difference $\eta \equiv (\rho - \rho')/\rho$. Ellison & Turner (1959) found that in an almost-parallel flow the entrainment constant ϵ was a function of the Richardson number $Ri \equiv \eta g L/U^2$, where L and U are typical length and velocity scales. In the present situation the flows are assumed to be self-similar, and all geometrical length scales are proportional to the radial distance r. Taking $U = q$ as a typical velocity, we see that $Ri \propto \eta g r/q^2$, which is independent of r. Hence we may be justified in assuming C to be a constant independent of r, though depending in some way on the relative density difference η, and the geometry of the flow.

Following the method of § 3 we find in place of (3.22)

$$E = -\frac{3CQ}{\sin 3\delta}\frac{\rho}{\rho'}, \quad F = \frac{3CQ}{\sin \delta}\frac{\rho}{\rho'} \tag{5.1}$$

† It is possible that this flow approximates the flow near the *crest* of a spilling breaker.

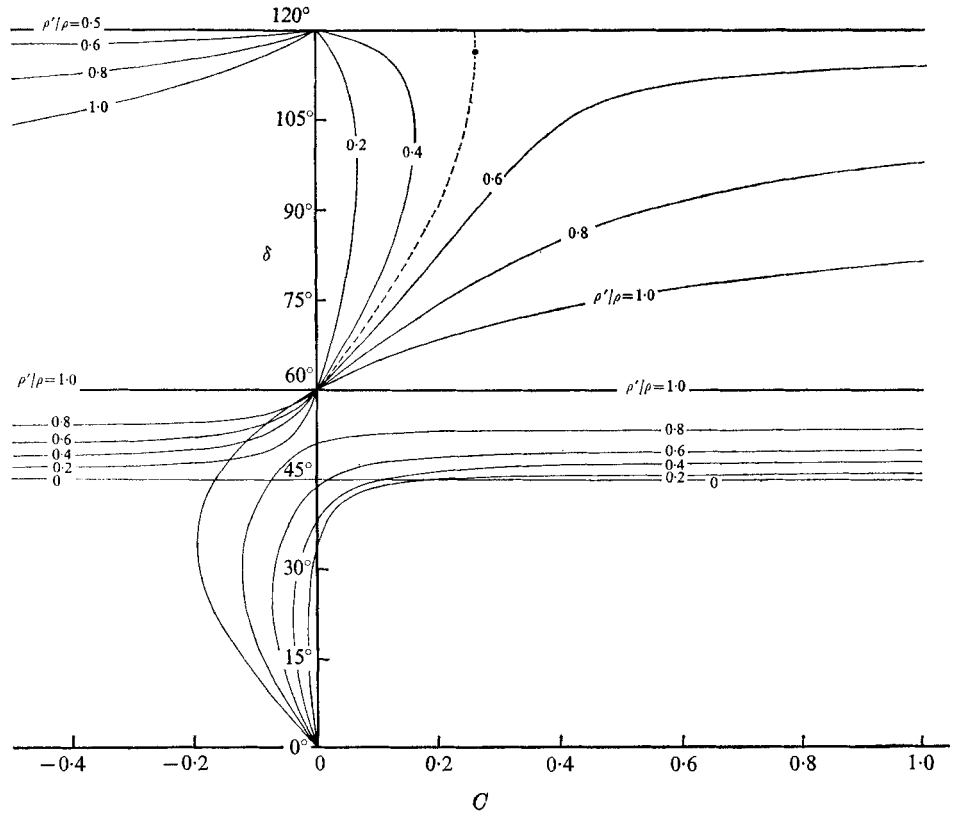

FIGURE 7. The angle δ shown as a function of C, for given values of the density ratio ρ'/ρ. The dashed line corresponds to $\rho'/\rho = 0{\cdot}5$. The maximum value of C on this curve is indicated by a solid circle (●).

and in place of (3.23) and (3.24)

$$\left.\begin{aligned}(\cot 3\delta - \cot\delta) &= \frac{1}{3C}\left(1-\eta\frac{\cos\beta}{\cos\alpha}\right),\\ (\operatorname{cosec} 3\delta - \operatorname{cosec}\delta) &= \frac{1}{3C}(1-\eta)\frac{\cos\gamma}{\cos\alpha},\end{aligned}\right\} \tag{5.2}$$

where $$\eta = (\rho-\rho')/\rho = 1-R, \qquad R = \rho'/\rho. \tag{5.3}$$

By eliminating α and C respectively from equations (5.2)

$$C = -\frac{(1-\eta)}{6}\frac{\sin 3\delta\,[\sin(\delta-\frac{1}{3}\pi)+\eta\sin\delta]}{(1-\eta)\cos\delta\sin(\delta-\frac{1}{3}\pi)} \tag{5.4}$$

and $$\tan\gamma = \frac{(\sin 2\delta+\sqrt{3})\sin(\delta-\frac{1}{3}\pi)+2\eta\cos\delta\sin^2\delta}{\cos 2\delta\,[\sin(\delta-\frac{1}{3}\pi)+\eta\sin\delta]}, \tag{5.5}$$

which are obviously generalizations of (4.2) and (4.7). For any given value of η we now have C and γ in terms of δ, so that α, β, γ and δ may all be expressed as functions of C.

In figure 7, δ is shown as a function of m over the whole possible range

$$0 \leqslant \delta \leqslant 120°.$$

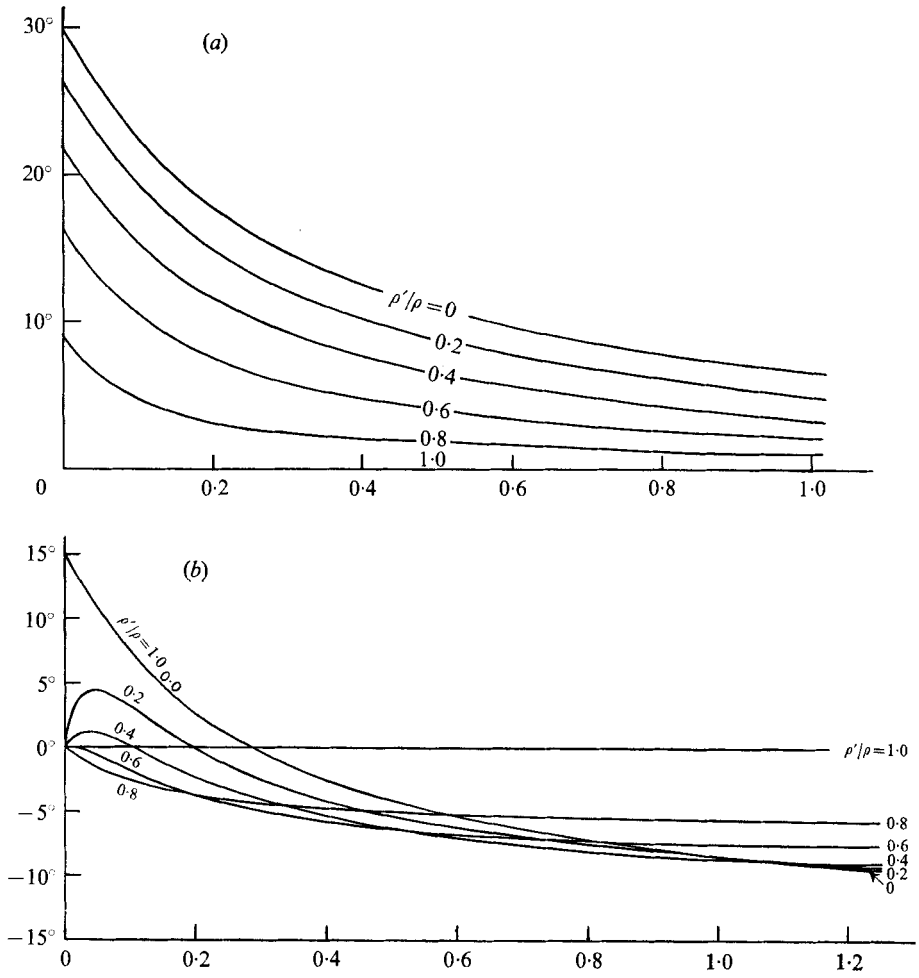

FIGURE 8. Values of α' and γ' for the quasi-static flows ($\delta' < 0$), giving the inclination of the free surface in the laminar and the turbulent zones respectively.

In fact we are interested only in positive values of C, and this limits the relevant values of δ to two ranges, (1) when $30° < \delta < 60°$ and (2) when $60° < \delta < 120°$.

In range 1, C can tend to zero for values of δ given by

$$\sin(\delta - \tfrac{1}{3}\pi) + \eta \sin\delta = 0. \tag{5.6}$$

At such values both E and F vanish, by (5.1), so that the fluid on the left is static. From (5.5) we may verify that in this case $\gamma = 90°$, hence $\delta = 90° - \beta$ and (5.6) reduces to (2.11). Thus in the limit as $C \to 0$ we recover the flows described in § 2. As C is increased, keeping δ within the range 1, we obtain a set of flows which are generalizations of the flows in § 2. The tangential stress at the interface no longer vanishes. It can be seen from figure 7 that these more general flows are continuous with those corresponding to points on the line $\delta = 60°$ ($\delta' = 0$) as $R \to 1$ ($\eta \to 0$) which correspond to a state of rest in *both* the laminar and turbulent zones. For this reason we may call the flows in range 1 'quasi-static' flows. For

such flows we see that δ' $(= \delta - 60°)$ is negative, so that the free surface is convex.

The values of α' and γ' corresponding to the quasi-static flows are shown in figures 8 (*a*) and (*b*). It will be seen that as R is diminished from unity, keeping C constant, so the angle of depression α' on the right generally increases, as we might expect, though the behaviour of γ' is more complicated. In the limit as $R \to 0$ and $C \to 0$, we see that $\alpha' \to 30°$, so that the flow on the right is the Stokes 120° angle flow, as we should expect. However, the flow on the left depends on the way in which C and R each tend to zero. Such non-uniform convergence is to be expected, since the ratio of the tangential stress to normal stress in the turbulent fluid depends on the ratio $C\rho/\rho'$; that is, C/R.

Consider now the flows in range 2 ($60° < \delta < 120°$). From figure 9 it can be seen that these are continuous with the flows described in §§ 3 and 4. We shall call the flows in this range 'dynamic'. For dynamic flows C may not tend to 0 unless either $\delta \to 60°$ or 120°, or unless $R \to 0$. There is a critical ratio of the densities: $R = 0{\cdot}5$. When $R > 0{\cdot}5$, then C becomes arbitrarily large as δ approaches a certain value. On the other hand, when $R \leqslant 0{\cdot}5$, C cannot exceed a certain maximum value, depending on R.

When $R = 0{\cdot}5$ the maximum value of C occurs at $\delta = 116° 30'$, which is inside the range 2. Hence there exists a small range of the density ratio, say

$$0{\cdot}5 < R < R_0,$$

for which C has *two* stationary values. Thus we see that when $0 < R < 0{\cdot}5$ there are generally two dynamic flows or none, for a given value of C; when $0{\cdot}5 < R < R_0$ there are either three dynamic flows or one; and when $R_0 < R \leqslant 1$ there is always just one flow for a given value of C.

An approximate method (not described here) shows that the value of R_0 is roughly $\frac{1}{2}(1+\zeta)$, where $\zeta = (2/135)^2 = 0{\cdot}00022$. Hence $R_0 \doteqdot 0{\cdot}50011$. By direct computation using (5.4) it was found that in fact $R_0 = 0{\cdot}500117\ldots$. The corresponding values of α', β', γ' and δ' are given by

$$\left.\begin{aligned} \alpha' &= 3° 23', \quad \beta' = 56° 37', \\ \gamma' &= 1° 54', \quad \delta' = 57° 42', \end{aligned}\right\} \tag{5.7}$$

and C has the value 0·26146.

The general values of α' and γ' for the dynamic flows are shown in figures 9 (*a*) and (*b*). At moderate values of C it appears that, as R is diminished from unity, so α' and γ' both initially increase. For example, if C is of order 0·1, then a change of 10 % in the ratio R, from 1·0 to 0·9, will increase α' by about 5° and will increase γ' by about 8°. At very low densities (small values of R) if C also is sufficiently small, α' must tend to 30°, so that we retrieve the Stokes 120° angle. At the same time γ' lies somewhere between 30° and 60°.

6. Comparison with observations

There appear to be few existing measurements with which the present model can be directly compared. Hydraulic jumps in open channels have been fairly

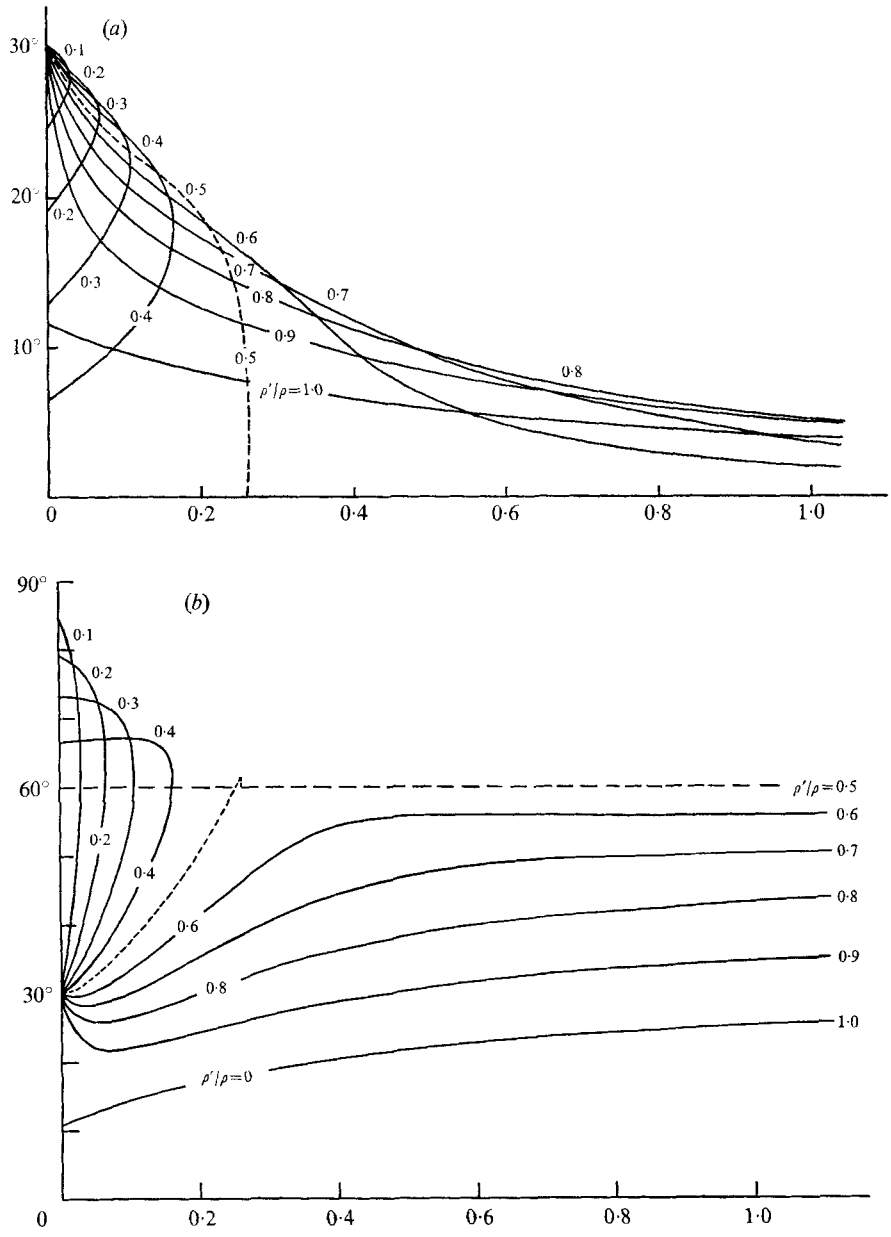

FIGURE 9. Values of (*a*) α' and (*b*) γ' for the dynamic flows ($\delta' > 0$), giving the inclination of the free surface in the laminar and the turbulent zones respectively.

extensively studied (for a review see Rajaratnam 1967). In these, however, the flow is strongly influenced by the presence of the bottom, especially at high Froude numbers. Nevertheless, some comparisons may be made. Bakhmeteff & Matzke (1936) showed that the profile of the hump was dependent on the Froude number $F_1 = U_1/(gh_1)^{\frac{1}{2}}$, where U_1 and h_1 denote the mean velocity and water depth below the jump. From figure 2 of Rajaratnam (1968), based on their data,

F_1	$\tan\gamma'$	γ'
1·98	0·59	29°
2·92	0·44	24°
4·09	0·39	21°
5·53	0·26	15°
8·63	0·23	13°

TABLE 1. Inclination of the free surface above the toe of a hydraulic jump in open channel flow.

the inclination of the free surface just above the toe of the jump is given by table 1. Comparison with figure 9(*b*) shows that these inclinations, in the range 13–29°, might be expected on the basis of an entrainment coefficient C of order 0·1 and a density ratio lying in the range $0{\cdot}7 < \rho'/\rho < 1{\cdot}0$.

Air entrainment in hydraulic jumps has been studied by Rajaratnam (1962). The volume concentration c, as defined by him, is approximately equal to $1-\rho'/\rho$. Over a comparable range of Froude numbers ($2{\cdot}42 \leqslant F_1 \leqslant 8{\cdot}12$) he found that, for points near the upper surface, c lay generally between 0·5 and 0·20. No measurements very close to the toe of the jump are reported, but the trend of the observations suggested that the air concentration there was even higher. Thus, the density ratio ρ'/ρ was certainly sometimes as low as 0·8 and may well have been less. The range of densities inferred earlier is therefore reasonable.

There appear to be no careful observations of the lower interface of the air-entrained flow. Rajaratnam (1967, p. 218) states that the angle of depression of the entrained bubbles increases with the Froude number. This may be due partly to the increase in the mean flow velocity, relative to the rate at which bubbles rise to the surface. Generally, interfacial angles indicated by air-bubble entrainment will tend to underestimate the actual angle of depression. Again, the presence of the bottom will tend to diminish the apparent angle of depression, except perhaps very close to the toe, and to reduce the range of validity of the local solution.

Immediately upstream of the toe it has been generally assumed, on the basis of nonlinear hydrostatic theory, that the free surface is exactly horizontal. However, in the neighbourhood of a discontinuity of surface elevation the hydrostatic assumption does not necessarily apply. Figure 9(*a*) suggests that close to the toe the free surface will be inclined to the horizontal at an angle α' lying between about 10° and 20°. Such small angles may have been overlooked.

7. Discussion and applications

In the foregoing model it has been assumed for simplicity that both N and C are constant. The fact that the resulting flow field is independent of the value of N suggests that the velocity of the model does not depend critically on the constancy of N. Nevertheless we may note that comparable analytic solutions could be obtained if N were assumed proportional to a power of the radial distance r; for example, if $N \propto g^{\frac{1}{2}}r^{\frac{3}{2}}$.

It must be emphasized that the representation of the turbulence by an eddy viscosity is necessarily an analytical device, made necessary by the complication of the actual flow. The chief significance of the present model may be to suggest a way in which the hitherto intractable problem of white-caps may be made amenable to analysis, namely by treating certain regions of the flow as laminar and others as turbulent, the turbulence being represented by an eddy viscosity, uniform or otherwise.

For example, it may well be possible to construct a solution for a spilling breaker in which the white-cap is represented by a viscous zone near the wave crest, the eddy viscosity diminishing towards the rear, as in figure 1. Because of the dissipation of energy it would be necessary, in an exactly steady state, to assume that energy was continually being supplied by normal or tangential stresses at the free surface.

In deep water the waves may be supposed to move forwards through a wave group, thus changing slowly in amplitude. Such a solution might be considered as quasi-stationary. If, on the other hand, the waves are in shallow water approaching a gently sloping beach, the energy is supplied by the incoming swell.

I am indebted to Dr J. S. Turner for comments on a first draft of this paper, and to Mr I. D. James for checking the algebra in §5.

REFERENCES

BAKHMETEFF, B. A. & MATZKE, A. E. 1936 The hydraulic jump in terms of dynamic similarity. *Trans. A.S.C.E.* **101**, 630–680.

DAVIES, T. V. 1952 Symmetrical, finite amplitude gravity waves. In *Gravity Waves*, pp. 55–60. U.S. Nat. Bur. Standards. Circular no. 521.

DIVOKY, D., LE MÉHAUTÉ, B. & LIN, A. 1970 Breaking waves on gentle slopes. *J. Geophys. Res.* **75**, 1681–1692.

DONELAN, M., LONGUET-HIGGINS, M. S. & TURNER, J. S. 1972 Periodicity in white-caps. *Nature*, **239**, 449–451.

ELLISON, T. H. & TURNER, J. S. 1959 Turbulent entrainment in stratified flows. *J. Fluid Mech.* **6**, 423–448.

GALVIN, C. J. 1967 Longshore current velocity: A review of theory and data. *Rev. Geophys.* **5**, 287–304.

IPPEN, A. T. & KULIN, G. 1955 Shoaling and breaking characteristics of the solitary wave. *M.I.T. Hydrodynamics Lab. Rep.* no. 15.

IVERSON, H. W. 1952 Laboratory study of breakers. In *Gravity Waves*, pp. 9–32. U.S. Nat. Bur. Standards. Circular no. 521.

LAMB, H. 1932 *Hydrodynamics*, 6th edn. Cambridge University Press.

LONGUET-HIGGINS, M. S. 1969*a* On wave breaking and the equilibrium spectrum of wind-generated waves. *Proc. Roy. Soc.* A **310**, 151–159.

LONGUET-HIGGINS, M. S. 1969*b* A non-linear mechanism for the generation of sea waves. *Proc. Roy. Soc.* A **311**, 371–309.

LONGUET-HIGGINS, M. S. 1970*a* Longshore currents generated by obliquely incident sea waves, 1. *J. Geophys. Res.* **75**, 6778–6789.

LONGUET-HIGGINS, M. S. 1970*b* Longshore currents generated by obliquely incident sea waves, 2. *J. Geophys. Res.* **75**, 6790–6801.

MCCOWAN, J. 1894 On the highest wave of permanent type. *Phil. Mag.* **39**, 351–359.

MASON, M. A. 1952 Some observations of breaking waves. In *Gravity Waves*, pp. 215–220. U.S. Nat. Bur. Standards. Circular No. 521.

MICHE, R. 1944 Mouvements ondulatories de la mer en profondeur constante ou décroissante. *Ann. Ponts et Chaussées*, **114**, 25–87, 131–164, 270–292, 396–406.

MICHELL, J. H. 1893 The highest waves in water. *Phil. Mag.* **36**, 430–437.

MONAHAN, E. C. 1971 Oceanic whitecaps. *J. Phys. Oceanogr.* **1**, 139–144.

PHILLIPS, O. M. 1966 *The Dynamics of the Upper Ocean.* Cambridge University Press.

RAJARATNAM, N. 1962 An experimental study of the air entrainment characteristics of hydraulic jump. *J. Inst. Engng India*, **42**, 247–273.

RAJARATNAM, N. 1967 Hydraulic jumps. *Advances in Hydroscience*, vol. 4, pp. 197–280. Academic.

RAJARATNAM, N. 1968 Profile of the hydraulic jump. *Proc. A.S.C.E.* HY **3**, 663–673.

STEWART, R. W. & GRANT, H. L. 1962 Determination of the rate of dissipation of turbulent energy near the sea surface in the presence of waves. *J. Geophys. Res.* **67**, 3177–3180.

STREET, R. L. 1972 Shoaling of finite-amplitude waves on plane beaches. *Proc. 12th Conf. on Coastal Engng*, pp. 345–361. New York: A.S.C.E.

STOKES, G. G. 1880 On the theory of oscillatory waves, Appendix **B**. *Math. & Phys. Papers*, **1**, pp. 225–228. Cambridge University Press.

TURNER, J. S. 1969 Buoyant plumes and thermals. *Ann. Rev. Fluid Dyn.* **1**, 29–44.